Available online at www.sciencedirect.com
SCIENCE DIRECT

Journal of Sound and Vibration 262 (2003) 45–64

JOURNAL OF SOUND AND VIBRATION

www.elsevier.com/locate/jsvi

Adaptive harmonic wavelet transform with applications in vibration analysis

B. Liu

Temasek Laboratories and Centre for Wavelets, Approximation and Information Processing, National University of Singapore, 2 Science Drive 2, Singapore 117543, Singapore

Received 6 September 2001; accepted 17 June 2002

Abstract

An adaptive harmonic wavelet transform is developed by taking advantage of the flexibility of the generalized harmonic wavelets. It first constructs a partition tree, which contains a great number of disjoint partitions of the frequency axis of a signal with each corresponding to an orthogonal harmonic wavelet basis. Then it searches the tree for the partition to represent the signal most sparsely. Since the corresponding basis is adapted to the composition of the signal, the transform can well reveal its characteristics. This is demonstrated with analysis examples of some simulated and vibration signals as well as comparisons with the conventional orthogonal harmonic wavelet transforms and wavelet packet transform.

1. Introduction

The classical harmonic wavelet transform (HWT) was developed by Newland in 1993 [1]. Similar to the ordinary discrete wavelet transform [2,3], the classical HWT can also perform multiresolution analysis of a signal. In addition, it has a fast algorithm based on FFT for numerical implementation. A distinct advantage of harmonic wavelets is that they are disjoint in frequency. This, though having a trade-off of a relatively poor time localization, is desirable in the application situations where frequency analysis accuracy is of particular concern. In 1994, Newland [4,5] extended the classical harmonic wavelets to the generalized harmonic wavelets, which provide a great deal of freedom for signal representation yet retaining the advantages of the classical harmonic wavelets. By appropriately choosing the level parameters of the wavelets, Newland obtained the so-called musical wavelets which give a finer frequency resolution than the classical harmonic wavelets. In more recent years, Newland has further exploited the principle of

E-mail address: tslliub@nus.edu.sg (B. Liu).

0022-460X/03/$ - see front matter
PII: S0022-460X(02)01027-1

harmonic wavelets and applied the results to analysis of non-stationary sound and vibration signals [6–9].

HWT has recently drawn a considerable attention in different areas including biomedical signal processing [10–12], pattern recognition [13], dynamic modelling of non-linear partial differential equations [14], etc. In particular, in sound and vibration analysis, HWT has been applied with success by a number of researchers. Besides Newland as mentioned above, Chancey et al. [15], for example, found that HWT is powerful in handling the vibration transients generated in rotating machinery. In Ref. [16], Samuel et al. showed that the non-stationary metric defined in the domain of harmonic wavelets is more reliable than some commonly used metrics such as kurtosis in the fault detection of helicopter gearboxes. Bonel-Cerdan and Nikolajsen [17] and Chettri et al. [18] described the advantages of HWT over spectrum analysis and discussed the usefulness of HWT in machine vibration analysis. In a comparative study with short-time Fourier transform, Tang [19], on the other hand, showed the limitation of HWT in handling exponentially time-decaying signals, which may result from the time localization problem mentioned above.

Compared with the above studies, adaptive analysis using harmonic wavelets has received less attention. In fact, the generalized harmonic wavelets can form a great number of orthogonal bases, each of which is capable of representing a signal of finite energy completely. In other words, using the generalized harmonic wavelets, one can represent a signal in many different ways. This gives rise to the questions: what is and how can we choose the best way for a given signal? The present research addresses this problem and develops a method of adaptive harmonic wavelet transform (AHWT). We first introduce the concept of partition tree. It provides numerous choices to partition the frequency axis of a signal and each of the partitions corresponds to an orthogonal harmonic wavelet basis. Then we present an algorithm, which is an extension of the "best basis" algorithm used in wavelet packet transform [20], to search the tree for the partition and basis that yield the sparsest representation of the signal. As will be seen later, the selected basis is well adapted to the composition of the signal and can reveal its characteristics effectively.

The paper is organized as follows: In the next section, the theory of harmonic wavelets is reviewed briefly. The method of AHWT is then presented in Section 3 with discussions on some related issues. In Section 4, this method is applied to the analysis of some simulated signals and vibration data collected from a gearbox. Comparisons with the conventional orthogonal harmonic wavelet transforms and wavelet packet transform are also presented. Concluding remarks are finally given in Section 5.

2. Harmonic wavelets

2.1. The principle

The basic idea behind HWT is to analyze a signal with a wavelet whose spectrum is confined exactly to a frequency band [4]. Deriving from the Fourier transform

$$W_{m,n}(\omega) = \begin{cases} \dfrac{1}{(n-m)2\pi}, & m2\pi \leqslant \omega < n2\pi, \\ 0 & \text{otherwise}, \end{cases} \tag{1}$$

Newland obtained the following harmonic wavelet:

$$w_{m,n}(t) = \frac{\exp(\mathrm{i}n2\pi t) - \exp(\mathrm{i}m2\pi t)}{\mathrm{i}2\pi(n-m)t}, \tag{2}$$

where m and n are the level parameters and $1/(n-m)$ determines the scale of the wavelet. m and n are real and positive but not necessarily integers. It can be seen that $w_{m,n}(t)$ is complex-valued.

If we translate $w_{m,n}(t)$ by step $k/(n-m)$, where k is an integer, then we obtain the following translated harmonic wavelet:

$$w_{m,n,k}(t) = \frac{\exp[\mathrm{i}n2\pi(t - k/(n-m))] - \exp[\mathrm{i}m2\pi(t - k/(n-m))]}{\mathrm{i}2\pi(n-m)(t - k/(n-m))}. \tag{3}$$

The Fourier transform of $w_{m,n,k}(t)$ is given by

$$W_{m,n,k}(\omega) = \begin{cases} \frac{1}{(n-m)2\pi}\exp\left(-\mathrm{i}\omega\frac{k}{n-m}\right), & m2\pi \leqslant \omega < n2\pi, \\ 0 & \text{otherwise}, \end{cases} \tag{4}$$

which has the same modulus as $W_{m,n}(\omega)$ in Eq. (1).

Eq. (4) shows that $W_{m,n,k}(\omega)$ is identically zero except in the frequency band from $m2\pi$ to $n2\pi$ within which its modulus is constant. In addition, the Fourier transforms of the wavelets at adjacent frequency bands do not overlap each other. These properties make harmonic wavelets particularly useful when the accuracy of frequency analysis is of particular concern.

Eqs. (1) – (4) give the definition of the generalized harmonic wavelets. If the level parameters are specified as $m = 2^j$ and $n = 2^{j+1}$, they will reduce to the classical form of harmonic wavelets. The spectra of the classical harmonic wavelets are confined exactly to octave bands [1]. They are therefore well suited for characterizing a signal composed of high-frequency components of short duration plus low-frequency components of long duration but do not necessarily work well for others. The generalized harmonic wavelets provide the possibility to overcome this shortcoming.

In Ref. [4], Newland showed that if the pairs m and n begin with a pair for which $m = 0$ and continue with touching but not overlapping pairs to positive infinity, then the wavelets generated by Eqs. (3) and (4) and their complex conjugates provide a complete set of orthogonal basis functions for expanding any arbitrary function of finite energy. As an example, Newland proposed the so-called musical wavelets [4], which give a finer frequency resolution than the classical harmonic wavelets.

In general, using the generalized harmonic wavelets, a signal $f(t)$ can be represented as follows:

$$f(t) = \sum_{m,n}\sum_{k=-\infty}^{\infty}\{a_{m,n,k}w_{m,n,k}(t) + \tilde{a}_{m,n,k}\bar{w}_{m,n,k}(t)\}, \tag{5}$$

where $\bar{w}_{m,n,k}(t)$ is the complex conjugate of $w_{m,n,k}(t)$, and the complex wavelet coefficients

$$a_{m,n,k} = (n-m)\int_{-\infty}^{\infty} f(t)\bar{w}_{m,n,k}(t)\,\mathrm{d}t, \tag{6}$$

and

$$\tilde{a}_{m,n,k} = (n - m) \int_{-\infty}^{\infty} f(t) w_{m,n,k}(t)\, dt. \tag{7}$$

For a real-valued signal, $\tilde{a}_{m,n,k} = \bar{a}_{m,n,k}$, the conjugate of $a_{m,n,k}$.

2.2. Discrete implementation

In discrete implementation of HWT, circular harmonic wavelets are used [1,4]. For the harmonic wavelet in Eq. (3), the corresponding circular wavelet is defined as

$$w^c_{m,n,k}(t) = \sum_{j=-\infty}^{\infty} w_{m,n,k}(t - j), \tag{8}$$

on a unit interval of t. Newland showed that

$$w^c_{m,n,k}(t) = \frac{1}{n-m} \sum_{q=m}^{n-1} \exp\left\{ i2\pi q \left(t - \frac{k}{n-m} \right) \right\}. \tag{9}$$

Differing from the previous subsection, m and n are integers here. The circular wavelets can faithfully model any discrete signal of finite energy [4]. Fig. 1 shows the real and imaginary parts of the circular harmonic wavelets at the selected levels and translations.

Eq. (9) shares many properties of discrete Fourier transform (DFT). This makes it possible to take advantage of FFT to implement discrete HWT [4]. Fig. 2 shows the procedure of Newland's

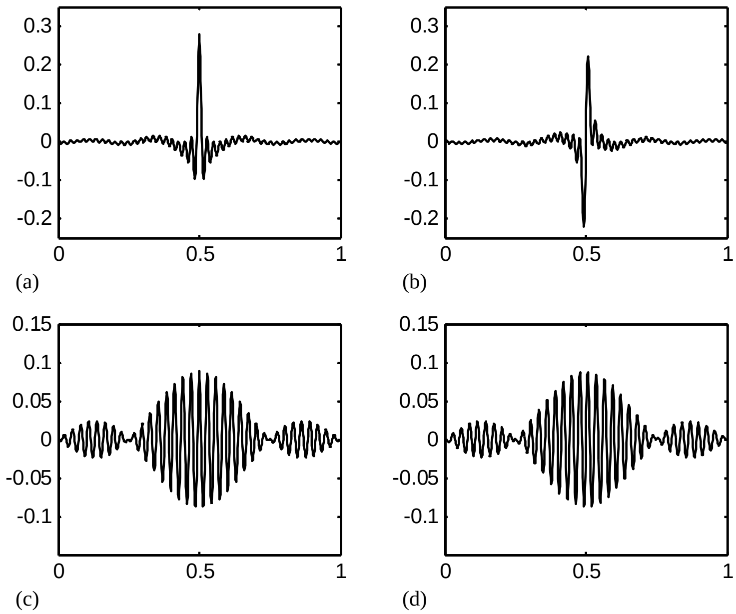

Fig. 1. Waveforms of circular harmonic wavelets: real part (a) and imaginary part (b) of the wavelet with $m = 5$, $n = 45$ and $k = 20$; real part (c) and imaginary part (d) of the wavelet with $m = 33$, $n = 37$ and $k = 2$.

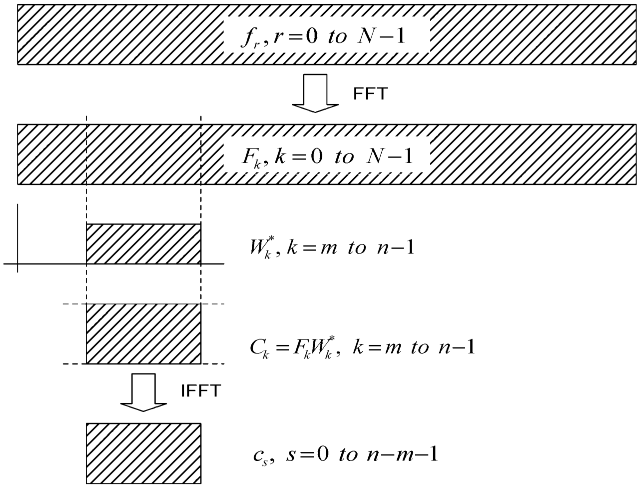

Fig. 2. Algorithm to compute harmonic wavelet coefficients for wavelets in the selected frequency band $m2\pi \leqslant \omega < n2\pi$ [6].

algorithm. It first applies FFT to the input signal, which is considered to be periodic in time with period 1. The decomposition coefficients of the wavelets in the frequency band $m2\pi$ to $n2\pi$ are then obtained by applying IFFT to the FFT restricted to this band. If the level parameters are specified as $m = 2^j$ and $n = 2^{j+1}$, then the algorithm implements the classical HWT of the signal. Similar to spectral analysis, for a real-valued signal, the decomposition coefficient of a wavelet above the Nyquist frequency is the complex conjugate of the decomposition coefficient of the corresponding wavelet in the interval from 0 to the Nyquist frequency. It is therefore only needed to consider the wavelets in this interval since those above the Nyquist frequency provide similar information.

The above algorithm provides a way to compute the decomposition coefficients of wavelets with predetermined level parameters. How to select the level parameters and hence the wavelets however remains a problem. Currently, this is often done empirically, which as discussed later has certain shortcomings. The proposed AHWT does the selection adaptively and overcomes the shortcomings.

3. Adaptive harmonic wavelet transform

In this section, the method of AHWT is presented. We will focus on dealing with real-valued discrete signals. The method however can be easily extended to the situation of complex-valued signals.

3.1. Partition tree

Harmonic wavelets provide a great deal of freedom to represent a signal. Choosing different sets of the level parameter pairs m and n in Eqs. (3) and (4) yields different representations.

Determining the set of the level parameter pairs for the signal is equivalent to selecting a disjoint partition of its frequency axis. In general, such a problem can be formulated as follows. Suppose that we have a real-valued discrete signal f of length N defined on the unit time interval $0 \leqslant t < 1$. Then according to Section 2.2, it is needed only to consider the DFT on the frequency sequence $\Omega = \{0, 2\pi, \ldots, k2\pi, \ldots, N_f 2\pi\}$ in decomposition of the signal, where $N_f 2\pi$ is the Nyquist frequency. Let $\{P_l\}_{l=0}^{L-1}$ be a disjoint partition of Ω, where $L \leqslant N_f + 1$ denotes the number of the frequency bands that the partition produces. Then, the DFT of the signal in each band $P_l = \{k2\pi\}_{k=m_l}^{m_{l+1}-1}$, with $m_0 = 0$ and $m_L = N_f + 1$, corresponds to a set of translated harmonic wavelets with an identical scale. The wavelets of all the frequency bands and their complex conjugates form an orthogonal basis and can represent the signal completely. Our problem is therefore to find the parameter set $\{L, m_1, \ldots, m_l, \ldots, m_{L-1}\}$ so that the corresponding wavelets can best represent the signal.

Finding the optimal solution to the above problem is generally not straightforward. We thus restrict our search for the solution to certain types of partitions. Specifically, we will consider those included in what we call a partition tree generated as follows. First, the frequency sequence Ω mentioned above, which is associated with the root node of the tree, is partitioned uniformly into a specified number of frequency bands. Each of these frequency bands corresponds to a node and is then further uniformly partitioned to generate the next level of the tree. In the situation where a frequency band is not divisible by the specified number, the partition can be roughly uniform. This process is continued until a specified level or the partition in which each band contains only one frequency is reached. It should be noted that the number of the frequency bands produced from different parent nodes are not necessarily the same. Clearly, the leaves of any connected subtree give a partition of Ω. According to Section 2, the corresponding harmonic wavelets and their complex conjugates form an orthogonal basis and can represent any signal of finite energy completely.

For the sake of convenience, we will use in the following the terminology "level 0" to denote the root level, and "level j", all the nodes obtained by partition of the frequency bands at "level $j-1$". This is different from Ref. [4] where "level m, n" is used when only one frequency band is considered. We will also use "node m, j" to represent the mth node at level j, where m starts from 0 and increases as the frequency increases. In addition, we will use L_j to denote the number of nodes at the jth level, and J, the level index of the bottom level.

A simple example of the partition tree is the binary tree illustrated in Fig. 3(a), where the root node corresponds to the DFT of the signal on Ω while each of the other nodes corresponds to a frequency band obtained by binary-splitting the frequency band associated with its parent node. This example is similar to wavelet packets [20,21]. However, the harmonic wavelet decomposition coefficients at different levels of the tree are all computed directly from the DFT of the signal while in wavelet packets, the coefficients in a children node are computed sequentially from the coefficients in its parent node. Figs. 3(b) and (c) give two more examples of the partition tree.

3.2. Selection of best partition

Given a partition tree, one has a huge number of disjoint partitions (e.g., more than $2^{2^{J-1}}$ for a binary tree [21]) to represent a signal. To choose the one that best represents a signal, we need first

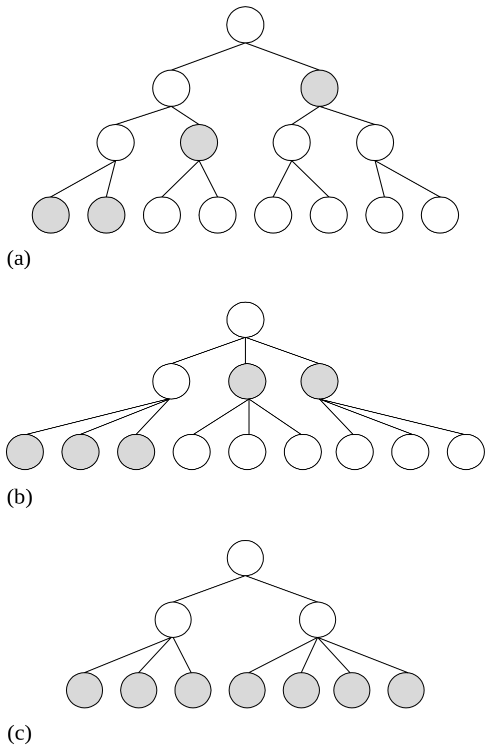

Fig. 3. Examples of partition tree: (a) a binary tree, (b) a ternary tree, and (c) a more complicated tree. The filled nodes in each figure correspond to an orthogonal harmonic wavelet basis.

a measure for evaluation of the quality of a representation, and second, an algorithm to search the tree for the partition that optimizes the measure.

In time–frequency analysis including wavelet transforms, sparsity is often used to evaluate the quality of a representation [21,22]. It means that the energy of the signal should be concentrated on as few basis functions as possible. Obviously, if every basis function in a representation has roughly the same decomposition coefficient, it is difficult to interpret the signal.

Among the various metrics of sparsity [20–22], we choose Shannon entropy as in Ref. [20] since it is an additive quantity and involves relatively low computation cost. For a sequence $x = \{x_i\}$, the Shannon entropy is defined as

$$H(x) = -\sum_i p_i \log p_i, \tag{10}$$

where $p_i = |x_i|^2/\|x\|^2$, and $p_{\mathrm{i}} \log p_i$ is set as 0 if $p_i = 0$. It can be shown that $H(x)$ is large if the elements of the sequence are roughly the same while small if all but a few elements are negligible [20,21,23].

To represent a signal with harmonic wavelets most sparsely, the partition selected from the partition tree should yield the decomposition coefficients that minimize the Shannon entropy over the tree. We call such a partition the "best partition" and following Refs. [20,21], the basis formed by the corresponding harmonic wavelets and their complex conjugates the "best basis".

Now we study how to search a partition tree for the best partition for a given signal and how to represent the signal with the best basis. In Ref. [20], Coifman and Wickerhauser proposed an algorithm to search the binary wavelet packet tree for the "best wavelet packet basis" to represent a signal most sparsely. In the following, we extend this algorithm to deal with our problem.

Suppose that we have a real-valued discrete signal f of length N defined on the unit time interval $0 \leqslant t < 1$. Then, selection of the best partition for f and representation of f using the corresponding best basis can be done as follows.

Step 1. Compute the FFT of the signal.

Step 2. Build the partition tree with the root node corresponding to the frequency sequence $\Omega = \{0, 2\pi, \ldots, k2\pi, \ldots, N_f 2\pi\}$,where $N_f 2\pi$ is the Nyquist frequency. Let $B_{m,j}$ be the partition with the original frequency band associated with node m,j being its only element, and $A_{m,j}$, the best partition of this frequency band, which is to be selected.

Step 3. Apply IFFT to the FFT restricted in the frequency band associated with each node to obtain the decomposition coefficients of the corresponding harmonic wavelets.

Step 4. Compute the entropy of the decomposition coefficient sequence associated with each node using Eq. (10) with $p_i = |c_i|^2/\|f\|^2$, where c_i are the decomposition coefficients. Denote by $H^B_{m,j}$ and $H^A_{m,j}$ the entropy corresponding to $B_{m,j}$ and $A_{m,j}$, respectively.

Step 5. Set $A_{m,J} = B_{m,J}$ and $H^A_{m,J} = H^B_{m,J}$ for $m = 0, 1, \ldots, L_{J-1}$.

Step 6. Determine the best partition $A_{m,j}$ for $j = J-1, J-2, \ldots, 0, m = 0, 1, \ldots, L_{j-1}$ as follows:
If $H^B_{m,j} \leqslant \sum_{n\in\Gamma_{m,j}} H^A_{n,j+1}$,
then $A_{m,j} = B_{m,j}$ and set $H^A_{m,j} = H^B_{m,j}$,
else $A_{m,j} = \cup_{n\in\Gamma_{m,j}} A_{n,j+1}$ and set $H^A_{m,j} = \sum_{n\in\Gamma_{m,j}} H^A_{n,j+1}$, where $\Gamma_{m,j}$ denotes the index set of the children nodes of node m,j.

Step 7. Represent the signal with the decomposition coefficients of the harmonic wavelets corresponding to the selected partition and their complex conjugates.

Following Ref. [20], one can easily show that for a given signal, the above algorithm yields the representation that has the minimum entropy over the prespecified partition tree. It is also clear that the algorithm is not restricted to only the analysis of the full frequency extent of a signal. If only a specific band is of concern, one can use the algorithm by building a partition tree (Step 2) whose root node is associated with this band rather than the full frequency extent. This will yield the sparsest representation for this frequency band. For example, vibration signals often contain some harmonic components whose frequencies are known, e.g., the rotating frequency of a machine. To deal with such components, harmonic basis functions are most suited. Therefore, in analysis of such signals, one may first retain the FFT values at the corresponding frequencies to represent the harmonic components, and then search for the sparsest representation using the above method for each of the frequency bands separated by the harmonic components.

3.3. Discussion

Currently, selection of the level parameters of the generalized harmonic wavelets is often done based on the *a priori* knowledge or by trial and error. For example, in vibration analysis, one may first select a frequency band that covers the frequencies of certain well-understood vibration events. The level parameters m and n in Eqs. (3) and (4) are then specified as the values that correspond to the lower and upper band limits. To reduce computation, this is often carried out only for the frequency bands of interest rather than the whole frequency range of the signal. While this approach works well sometimes, it has certain disadvantages in the general situation. First, in many cases, it is difficult to determine accurately the frequency range of a vibration event, such as the vibration excited by a localized gear defect. One may obtain some information with the help of spectral analysis. Such information however is unreliable because of the inability of spectral analysis in revealing the time characteristics of a signal. For example, a component that appears very small in the spectrum may dominate locally in time. The frequencies of such a component may be neglected if the analysis frequency band is determined based on spectral analysis. Second, this approach uses a fixed set of basis functions to represent the signal components that have the same frequency range but possibly different time–frequency compositions, and thus may not give the best representation for signal interpretation. In fact, to represent a set of near-harmonic components, wavelets of large scales are often desirable, while to represent transient components with the same frequency range, wavelets of small scales are generally more suited.

The proposed method overcomes the shortcomings mentioned above. Instead of using a fixed set of wavelets determined by the band limits, it selects different sets of wavelets adaptively to match the composition of different signals. In the situation where only a specific frequency band is of interest, one can either obtain the information from the AHWT for the full FFT spectrum or use the algorithm by building a tree for this band as mentioned previously. Even for the later, the proposed method does not require to estimate the frequency range of the analyzed vibration event accurately since the representation depends mainly on the composition of the signal itself rather than the band limits.

Compared with wavelet packet transform [20,21], the proposed AHWT provides more freedom in representing a signal in the sense that the construction of the partition trees is more flexible. This also provides a way to combine some prior knowledge about the characteristics of a signal with the proposed adaptive procedure. For example, as mentioned in the previous subsection, one may utilize the knowledge about the rotating frequencies of a machine to better represent a vibration signal. Owing to the properties of harmonic wavelets, the proposed method has a better capability in frequency analysis. This may be desirable in vibration analysis and some other application areas. On the other hand, wavelet packet transform theoretically has a higher analysis accuracy in time since the wavelets it uses has better time localization.

4. Applications

To demonstrate the performance of the proposed method, we present several application examples in this section.

4.1. Simulated examples

The purpose of the first example is to demonstrate the time–frequency analysis ability of the proposed AHWT and to investigate the influence of the choice of partition trees. We will compare our method with wavelet packet transform [20,21] as it is one of the most important adaptive orthogonal transforms for time–frequency analysis and has been applied in various areas including vibration analysis, e.g., Ref. [24]. The source codes used to implement wavelet packet transform for this example and the vibration analysis example in the next subsection is WaveLab, a wavelet analysis toolbox developed at Stanford University [25]. We consider a signal defined by

$$f(t) = \sin(152\pi t) + 0.8\sin(156\pi t) + 5\cos\left[0.56N\pi\left(t - \frac{229}{N}\right)\right]\exp\left\{-\left[\frac{N}{25}\left(t - \frac{229}{N}\right)\right]^2\pi\right\} + 4\cos\left[0.56N\pi\left(t - \frac{249}{N}\right)\right]\exp\left\{-\left[\frac{N}{25}\left(t - \frac{249}{N}\right)\right]^2\pi\right\}, \quad 0 \leqslant t < 1,$$

where $N = 512$ is the length of the signal. It consists of two harmonics and two modulated Gaussians spaced closely in frequency and time, respectively. Fig. 4 shows its waveform and Fourier transform, where A and B represent the two types of components in time, and A' and B', their corresponding spectrum.

We first analyze the signal using a binary partition tree. As can be seen from the time–frequency plane [21] in Fig. 5, the transform can well resolve the two modulated Gaussians as well as the two harmonics. The signal is then analyzed with wavelet packet transform. Daubechies wavelet db10 (length 20) is used as the filter [3]. The result is shown in Fig. 6. Compared with Figs. 4 and 5, it can be seen that wavelet packet transform has relatively low accuracy in frequency and cannot properly resolve the modulated Gaussians. For the two harmonics, it not only has a low-frequency resolution but also introduces considerable unexpected components, e.g., the one near 100π Hz. This is due to the overlap in frequency between wavelets of different bands although

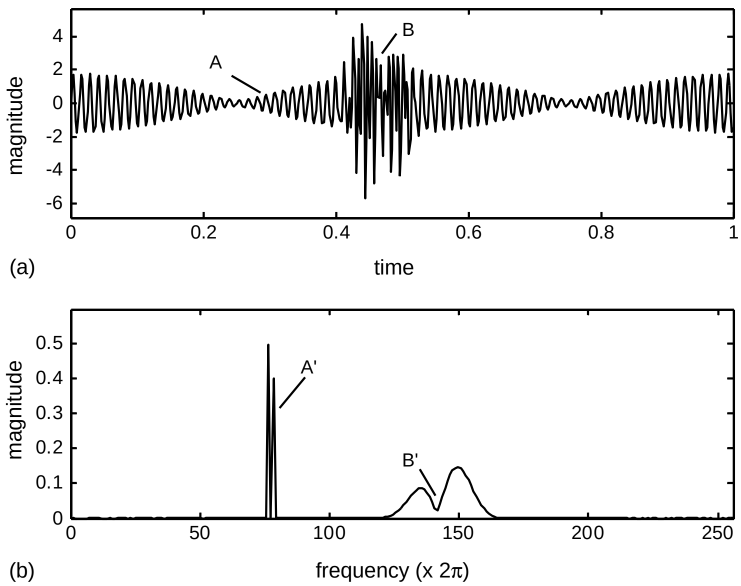

Fig. 4. (a) A simulated signal composed of two harmonics and two modulated Gaussians spaced closely in frequency and time, respectively, and (b) its Fourier transform.

wavelet db10 is rather localized in frequency in comparison with those of a short length. We have carried out more numerical experiments and found that the proposed method and wavelet packet transform may each have its advantages in analyzing the characteristics of a signal in time but the former usually works better in analyzing the characteristics in frequency. This can also been seen from the vibration analysis example given later.

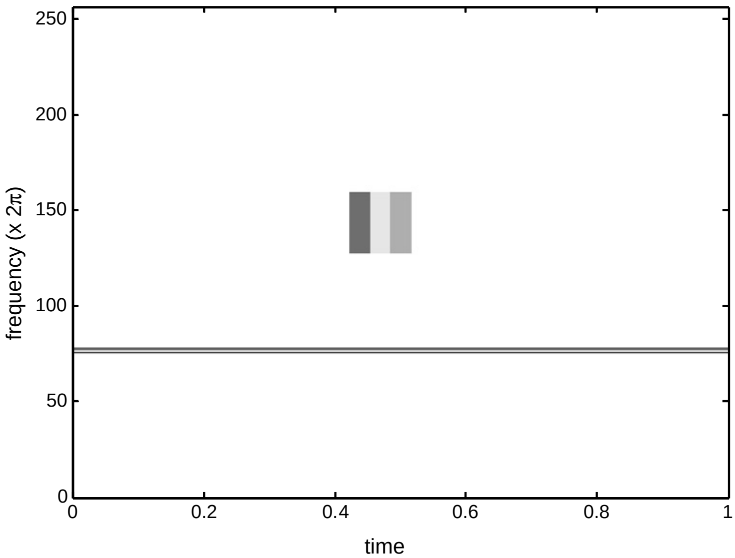

Fig. 5. Time–frequency plane of the signal in Fig. 4(a) obtained using AHWT with a binary tree.

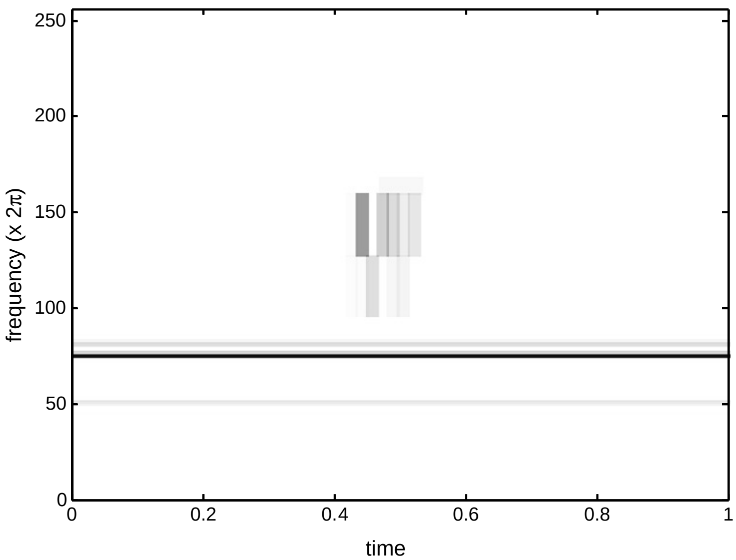

Fig. 6. Time–frequency plane of the signal in Fig. 4(a) obtained using wavelet packet transform.

Fig. 7 gives the analysis result obtained using a ternary partition tree. Compared with Fig. 5, it provides more information about the modulated Gaussians in frequency but cannot discriminate them in time. One can design a signal that yields a contrary result. This is because different trees contain different sets of harmonic wavelets. If a tree contains the wavelets that can well match the composition of a dominant signal component, it may have a high discrimination ability. Otherwise, the transform needs to employ more wavelets to represent the component and thus may result in a low analysis resolution. For the harmonics in the above signal, the ternary tree provides the same result as the binary tree. It should be pointed out that to obtain the best frequency resolution for harmonic components, it is generally required to partition the second maximum level of a tree in such a way that each of the produced nodes in the maximum level contains only one wavelet.

Based on the previous section, some trees may be included in some others. For example, a quaternary tree is included in a binary tree. This inclusion however does not mean that the quaternary tree is useless because the "simpler" partition it uses may sometimes produce a time–frequency plane that is "cleaner" and easier to interpret. In addition, a quaternary tree requires much less computation than a binary tree in decomposition of a signal. This is desirable in real-time applications or in the situation where the length of the signal is very large.

The second example is presented to demonstrate the feature detection ability of the proposed method. The simulated signal is defined by

$$f(t) = \sin(500\pi t) + 0.8\cos\left[0.6N\pi\left(t - \frac{511}{N}\right)\right]\sum_{k=0}^{3} s_k(t) + 0.2n(t), \quad 0 \leqslant t < 1,$$

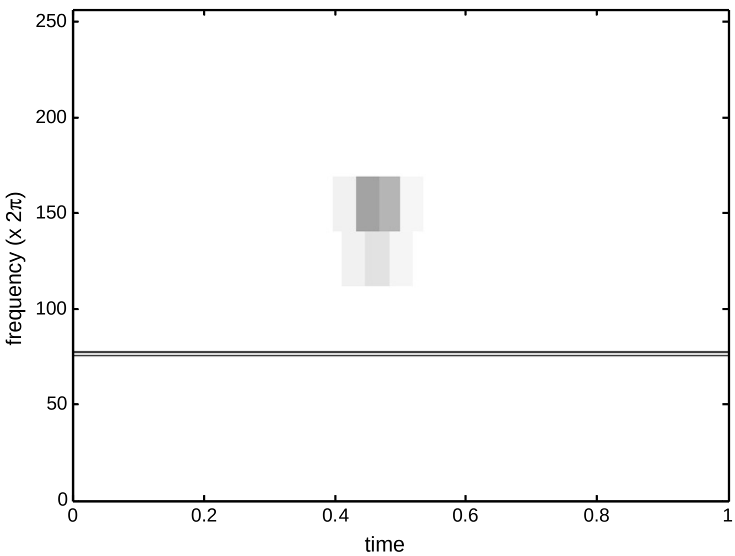

Fig. 7. Time–frequency plane of the signal in Fig. 4(a) obtained using AHWT with a ternary tree.

where

$$s_k(t) = \begin{cases} \exp\left[-\frac{N}{16}\sqrt{\pi}\left(t - \frac{119+250k}{N}\right)\right], & \frac{119+250k}{N} \leqslant t < 1, \\ 0, & 0 \leqslant t < \frac{119+250k}{N}, \end{cases}$$

$n(t)$ are standard normal variates, and $N = 1024$, the length of the signal. It consists of a sinusoid, four equally spaced one-sided modulated decaying exponentials and white noise. Similar compositions are often seen in vibration signals generated in rotating machines, such as rolling element bearings and gearboxes, with a local defect. In such a situation, the vibration at the rotating frequencies usually has a harmonic nature while that generated due to the defect often contains a sequence of transients. The purpose of the vibration analysis is often to detect the transients which usually have very small energy at the early stage of the failure development Figs. 8(a) and (b) show the waveform and Fourier transform of the simulated signal, respectively. A zoomed-in plot of the signal segment from the time instant 0.040 to 0.195 is given in Fig. 8(c). From the definition of the signal, we know that there is one modulated decaying exponential starting at the instant 0.116 (=119/1024) but we can hardly identify it from either the waveform or the spectrum. Fig. 9 shows the time–frequency plane obtained using the proposed algorithm

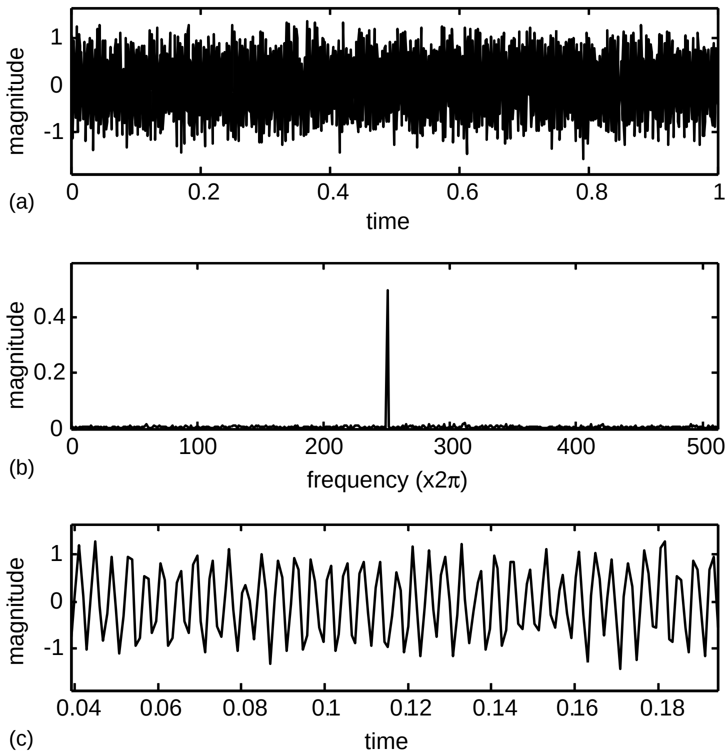

Fig. 8. (a) A simulated signal composed of a sinusoid, four equally spaced one-sided modulated decaying exponentials and white noise, (b) its Fourier transform, and (c) zoomed-in plot of the signal segment from the instant 0.040 to 0.195.

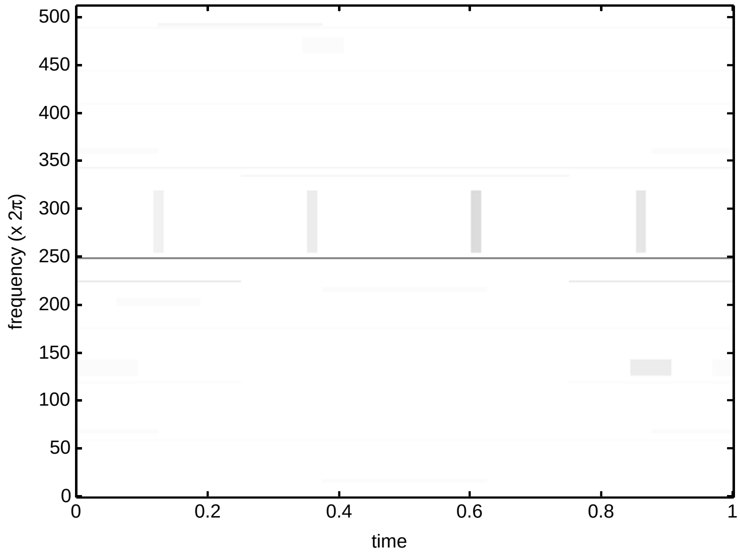

Fig. 9. Time–frequency plane of the signal in Fig. 8(a) obtained using AHWT with a binary tree.

with a binary tree. To properly observe both the sinusoid and the exponentials, logarithmic scale is used in representing the squared moduli of the decomposition coefficients. One can see clearly the sinusoid and the four modulated decaying exponentials as well as their time–frequency characteristics.

4.2. Vibration analysis

Now we present an application example of the proposed method in vibration analysis. The problem concerned in the example is gearbox failure detection. It is a typical topic of vibration monitoring and has been investigated using various methods including wavelet transform, e.g., Ref. [26]. In this paper, we will not investigate the details of the problem itself but focus more on illustration of the capability of the proposed method in vibration analysis. We will perform this by comparison with several related existing methods. In this subsection, logarithmic scale is used in representing the squared moduli of the decomposition coefficients in all the figures of time–frequency plane.

The vibration data used in the study were collected from a life testing experiment conducted on an automobile gearbox. The transmission gear train in the test was: Z28/Z48 → Z20/Z44 → Z30/Z36 → Z15/Z42. The rotation speed of the input shaft was 1600 r.p.m., i.e., 26.67 Hz. A load of 880 kg m was applied to the output shaft. At the end of the test, one tooth on the driving gear (Z15) of the last meshing pair was broken, which ran at 353.58 r.p.m., i.e., 5.89 Hz. The vibration signals were picked up at the bearing seat of the output shaft. They were lowpass-filtered at 1.8 kHz and then digitized with a sampling frequency of 4 kHz.

Fig. 10(a) shows a vibration signal picked up near the time when the tooth was broken, and Fig. 10(b), its Fourier transform. It is difficult to obtain clear information about the failure from

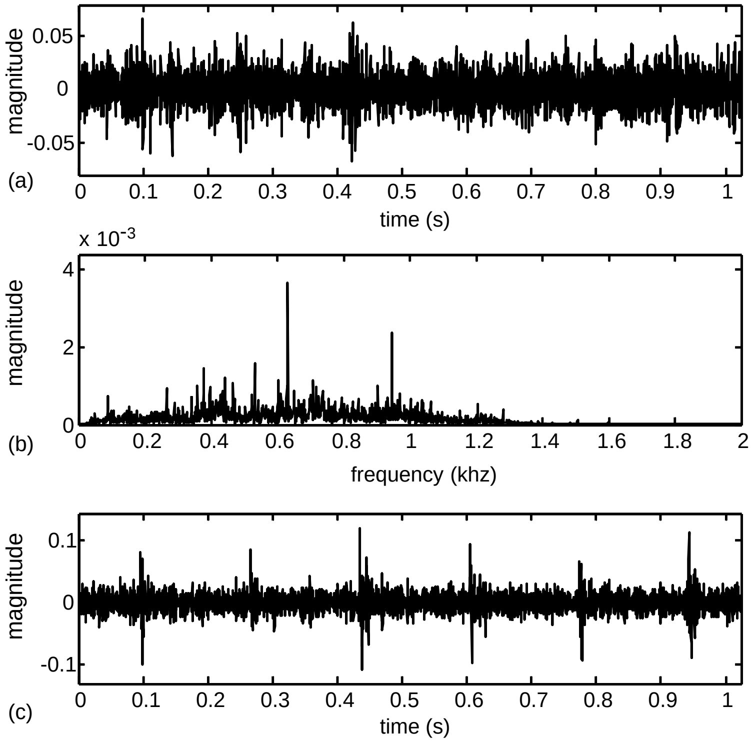

Fig. 10. (a) A vibration signal collected from the gearbox before the tooth breakage, (b) its Fourier transform, and (c) a vibration signal picked up after the tooth breakage.

the time record and the spectrum. For comparison, a signal picked up after the tooth was broken is given in Fig. 10(c), where there are regularly spaced impulses excited due to the breakage. Our purpose of vibration analysis is to detect the symptom before the breakage happens. This is of great importance in practice since tooth breakage in a gearbox may result in a catastrophic accident.

Fig. 11 shows the time–frequency plane of the signal in Fig. 10(a) obtained using the proposed method with a quarternary partition tree whose root node is associated with the whole band from 0 to the Nyquist frequency. One can see that in the frequency band from 125 to 250 Hz, there exist a sequence of regularly spaced dark patches. They have a short time duration but a relatively large frequency band and represent impulsive components in the signal. More importantly, the average time spacing between the neighbouring impulses is 0.166 s, corresponding to 6.02 Hz in frequency, which is very close to the rotation frequency of the damaged gear mentioned above. These features provide a clear indication about the condition of this gear. Compared with the spectrum in Fig. 10(b), the time–frequency plane also provides information about most of the harmonic components in the signal. For instance, one can see some near-harmonic components at the frequency of 88 Hz, which is close to 88.39 Hz, the meshing frequency of the last gear pair in the transmission path. Accurate representation of harmonic components is usually desirable in vibration analysis especially for vibration of rotating machinery.

Figs. 12 and 13 show the analysis results of the classical HWT and the musical wavelet transform. The former partitions the frequency axis into octave bands and the later further partitions each band above 32 Hz into 12 subbands to obtain a finer frequency resolution. In the band from 125 to 250 Hz, the classical HWT provides the same information as the proposed

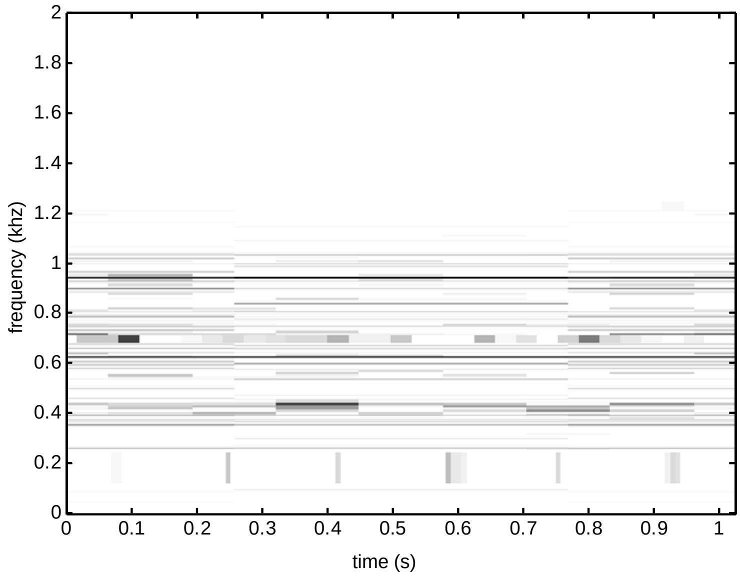

Fig. 11. Time–frequency plane of the signal in Fig. 10(a) obtained using AHWT with a quaternary tree.

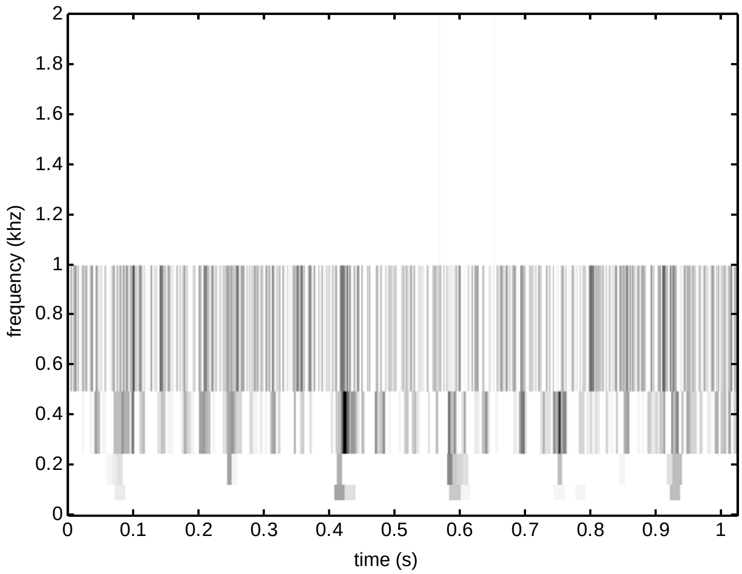

Fig. 12. Time–frequency plane of the signal in Fig. 10(a) obtained using the octave HWT.

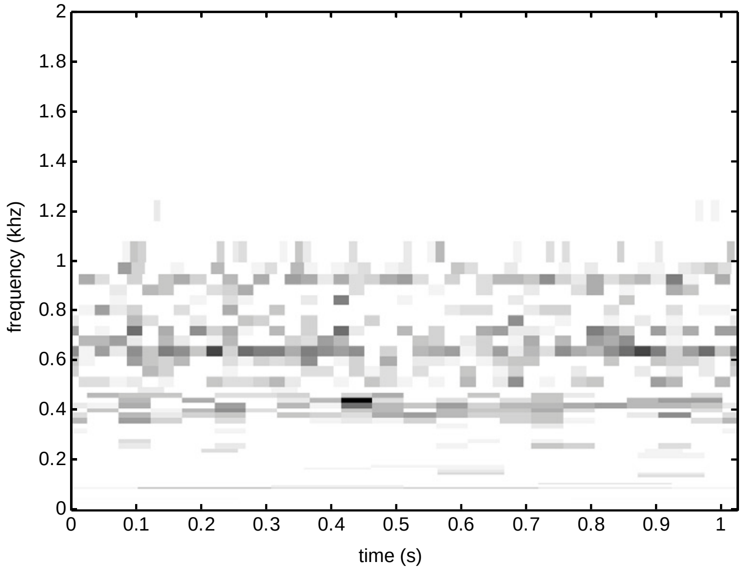

Fig. 13. Time–frequency plane of the signal in Fig. 10(a) obtained using musical wavelet transform.

AHWT and indicates clearly the presence of the failure. However, the representation it gives for other bands does not well reveal the characteristics of the signal. Owing to the octave nature, the classical HWT is mainly suited to deal with signals composed of high-frequency bursts plus low-frequency quasi-stationary components. As can be see from Fig. 13, the musical wavelet transform does not work well for the analyzed signal; its time resolution is too low to properly characterize the impulsive components in the above-mentioned band and its frequency resolution is not high enough to well represent most of the harmonics except for the meshing frequency of the last gear pair. We should point out that the partitions used in these two transforms are special cases included in the partition trees defined in the previous section.

Fig. 14 shows the result yielded by wavelet packet transform. Daubechies db8 (length 16) filter is used, which was found to be relatively effective compared with some other Daubechies filters in dealing with the given signal. As an adaptive approach, wavelet packet transform can effectively detect the impulses. It however cannot properly characterize the harmonic components in the signal. This again is due to the frequency overlap between wavelets of different bands. We have also analyzed the signal with wavelet packet transform using Symmlets and Coiflets [3] and obtained similar results. In comparison with Fig. 11, the proposed AHWT appears to be more effective.

5. Conclusion

In this paper, we have proposed an adaptive harmonic wavelet transform by exploiting the flexibility of the generalized harmonic wavelets. The basic idea behind this method is first to

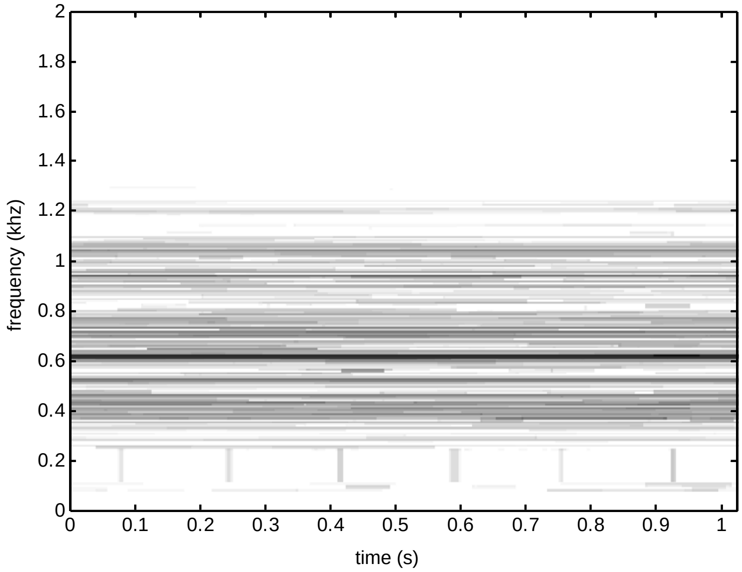

Fig. 14. Time–frequency plane of the signal in Fig. 10(a) obtained using wavelet packet transform.

construct a partition tree that includes numerous choices to partition the frequency axis of a signal and then to search the tree for the partition and hence the basis to represent the signal most sparsely. This basis is adapted to the composition of the signal and can well reveal its characteristics.

The proposed method was tested with analysis of simulated signals and vibration data of a gearbox. The results show that it performs better than the classical harmonic wavelet transform and musical wavelet transform, which use a fixed partition of the frequency axis and are suited only for certain types of signals. The proposed method also overcomes the shortcoming of the conventional approach of generalized harmonic wavelet transform that determines the level parameters of harmonic wavelets either based on prior knowledge or by trial and error. Compared with wavelet packet transform, the proposed method provides more freedom in representing a signal in the sense that the construction of the partition tree can be more flexible. The application examples also show that the proposed method works better than wavelet packet transform in frequency analysis. This makes it more suitable for dealing with vibration signals.

Harmonic wavelets have a high-frequency analysis accuracy but a relatively poor time localization. Although this drawback is not evident in our testing examples, it is needed to improve the time localization for more general application situations of adaptive analysis. Research on this topic is in progress.

Acknowledgements

The author would like to thank Assoc. Prof. X. Zhang, College of Mechanical Engineering, Xi'an Jiaotong University, China, for providing the gearbox vibration data used in the paper.

References

[1] D.E. Newland, Harmonic wavelet analysis, Proceedings of the Royal Society of London A 443 (1993) 203–225.
[2] S. Mallat, A theory for multiresolution signal decomposition: the wavelet representation, IEEE Transactions on Pattern Analysis and Machine Intelligence 11 (1989) 674–693.
[3] I. Daubechies, Ten Lectures on Wavelets, SIAM, Philadelphia, PA, 1992.
[4] D.E. Newland, Harmonic and musical wavelets, Proceedings of the Royal Society of London A 444 (1994) 605–620.
[5] D.E. Newland, Wavelet analysis of vibration, Part 1: theory, Part 2: wavelet maps, American Society of Mechanical Engineers Journal of Vibration and Acoustics 116 (1994) 409–425.
[6] D.E. Newland, Time–frequency and time-scale signal analysis by harmonic wavelets, in: A. Prochazka, J. Uhlir, P.J.W. Rayner, N.G. Kingsbury (Eds.), Signal Analysis and Prediction, Birkhauser, Boston, MA, 1998, pp. 3–26.
[7] D.E. Newland, Harmonic wavelets in vibrations and acoustics, Philosophical Transactions of the Royal Society of London A 357 (1999) 2607–2625.
[8] D.E. Newland, Ridge and phase identification in the frequency analysis of transient signals by harmonic wavelets, American Society of Mechanical Engineers Journal of Vibration and Acoustics 121 (1999) 149–155.
[9] D.E. Newland, Computation of time-varying cross-spectra, Proceedings of the Seventh International Congress on Sound and Vibration, July 4–7, Garmisch-Partenkirchen, Germany, Kramer Technology Publ., Munich, 2000, pp. 3447–3454.
[10] R.A. Bates, M.F. Hilton, K.R. Godfrey, M.J. Chappell, Autonomic function assessment using analysis of heart rate variability, Control Engineering Practice 5 (1997) 1731–1737.
[11] A. Batista, M. English, Ventricular late potential analysis with musical and harmonic wavelets, Medical Engineering & Physics 20 (1998) 773–779.
[12] M.F. Hilton, R.A. Bates, K.R. Godfrey, M.J. Chappell, R.M. Cayton, Evaluation of frequency and time–frequency spectral analysis of heart rate variability as a diagnostic marker of the sleep apnoea syndrome, Medical & Biological Engineering and Computing 37 (1999) 760–769.
[13] H. Drolon, F. Druaux, A. Faure, Particles shape analysis and classification using the wavelet transform, Pattern Recognition Letters 21 (2000) 473–482.
[14] S.V. Muniandy, I.M. Moroz, Galerkin modelling of the Burgers equation using harmonic wavelets, Physics Letters A 235 (1997) 352–356.
[15] V.C. Chancey, G.T. Flowers, C.L. Howard, Rotordynamic analysis using harmonic wavelets, Proceedings of the Seventh International Congress on Sound and Vibration, July 4–7, Garmisch-Partenkirchen, Germany, Kramer Technology Publ., Munich, 2000, pp. 3519–3526.
[16] P.D. Samuel, D.J. Pines, D.G. Lewicki, A comparison of stationary and non-stationary metrics for detecting faults in helicopter gearboxes, Journal of American Helicopter Society 45 (2000) 125–136.
[17] J.I. Bonel-Cerdan, J.L. Nikolajsen, Introduction to harmonic wavelet analysis of machine vibrations. Proceedings of the 1997 International Gas Turbine and Aeroengine Congress and Exposition, June 2–5, Orlando, FL, Paper 97-GT-58, 1997.
[18] S.R. Chettri, Y. Ishiwaka, H. Kimura, I. Nagano, Harmonic wavelets, constant Q transforms, and the cone kernel TFD, Proceedings of SPIE 2762 (1996) 446–451.
[19] S.K. Tang, On the time-frequency analysis of signals that decay exponentially with time, Journal of Sound and Vibration 234 (2000) 241–258.
[20] R.R. Coifman, M.V. Wickerhauser, Entropy-based algorithms for best basis selection, IEEE Transactions on Information Theory 38 (1992) 713–718.
[21] M.V. Wickerhauser, Adapted Wavelet Analysis from Theory to Software, A. K. Peters, Natick, MA, 1994.
[22] S.S. Chen, D.L. Donoho, M.A. Saunders, Atomic decomposition by basis pursuit, SIAM Review 43 (2001) 129–159.
[23] G. Silviu, Information Theory with Applications, McGraw-Hill, New York, 1977.

[24] G.G. Yen, K.C. Lin, Wavelet packet feature extraction for vibration monitoring, IEEE Transactions on Industrial Electronics 47 (2000) 650–667.
[25] D. Donoho, M.R. Duncan, X. Huo, O. Levi, J. Buckheit, M. Clerc, J. Kalifa, S. Mallat, T. Yu, WaveLab, v802, 1999, fttp://playfair.stanford.edu.
[26] W.J. Wang, P.D. McFadden, Application of wavelets to gearbox vibration signals for fault detection, Journal of Sound and Vibration 192 (1996) 927–939.